Available online at www.sciencedirect.com

ScienceDirect

IFAC PapersOnLine 56-2 (2023) 1478–1483

Neurofuzzy Defocusing strategy for a Fresnel collector

Adriano S. M. Brandão * **William D. Chicaiza** ** **Adolfo J. Sánchez** ***
Julio Elias Normey-Rico * **Juan M. Escaño** **

* *Universidade Federal de Santa Catarina - UFSC. Departamento de Automação e Sistemas. Florianópolis, SC, Brasil, (e-mail: adriano.brandao@posgrad.ufsc.br, julio.normey@ufsc.br).*
** *Departamento de Ingeniería de Sistemas y Automática, Universidad de Sevilla, Camino de los Descubrimientos s/n., 41092 Sevilla, Spain, (e-mail: wchicaiza@us.es, jescano@us.es)*
*** *Department of Mechanical, Biomedical, and Manufacturing Engineering, Munster Technological University. Bishopstown, Cork, Ireland, (e-mail: adolfo.sanchezdelpozofernandez@mtu.ie)*

Abstract: Concentrating Solar Power systems are widely applied as a means to utilize the sun's abundant renewable energy, but the design of these processes facilitates the occurrence of overheating. This work presents two approaches for calculating the mirror angles of a fresnel collector in order to limit the amount of solar energy collected. The proposed structures are designed to receive a desired focus value from a controller and generate references for the mirror inclination controllers of the collector. The first strategy consists of the use of an optimization problem coupled with a simplified model of the collector. Whereas, the second approach consists of an ANFIS network that is trained with data from a reliable collector model made in SolTrace®. Both approaches are compared with simulations in SolTrace® the results show that the ANFIS solution presented overall better results, taking into account error and computational time.

Keywords: Defocusing, Fresnel, Neuro-Fuzzy, Fuzzy Inference System, Optimization

1. INTRODUCTION

In solar energy applications, the main source of energy cannot be directly manipulated, making these processes particularly susceptible to weather disturbances. This limitation presents challenges for control systems, motivating research to increase the operational capabilities of this type of process (Camacho et al., 2012).

One of the main operational issues for Concentrating Solar Power (CSP) plants is the overheating of the Heat Transfer Fluid (HTF), which frequently occurs as the solar collector fields are designed to provide multiples of the thermal energy required for operation. If overheating temperatures are reached, the HTF can degrade, generating numerous issues, reducing the system's performance, and compromising its safety. Therefore, avoiding the maximum temperature limits is an interesting control problem, since the solar collector should provide the biggest energy output possible while maintaining the integrity of the process components.

Some works propose the use of defocusing of the solar collectors to prevent overheating. Sánchez et al. (2018) present a novel control strategy for the prevention of overheating of HTF by defocusing collectors on a commercial 50 *MW* parabolic trough plant model by means of a Gain Scheduling MPC. Elias et al. (2019) presented an ON/OFF defocus strategy as well as a partial defocus control strategy taking into account intermediate focus positions. Both approaches were applied on ACUREX parabolic troughs.

Many works utilize Neuro-Fuzzy techniques to model nonlinear of dynamic systems, control and estimation of solar concentration processes. For example, in Escaño et al. (2020) developed a soft sensor to classify the behavior of drivers in real time. The algorithm consists of several NF systems in combination with PCA. In addition, a Neurofuzzy estimator is developed in Escaño et al. (2021) to estimate the non-observable states in a parabolic trough solar field. In addition, Chicaiza et al. (2021, 2022) a Neurofuzzy model of a Fresnel solar field and high temperature generator (HTG) is developed, focusing on a rule-based model.

This work proposes a defocusing strategy for fresnel collectors, considering the collector's optical geometry in order to calculate the mirror inclination angles that produce the required focus value. Two contributions to the proposed strategy are compared: the first uses the model proposed by Brandão et al. (2022) in an optimization problem to determine the mirrors' angles, and the second consists of a Neurofuzzy structure that is trained with a reference ray-tracing software. Specifically SolTrace® software from NREL (Wendelin, 2003). Both implementations are compared with simulations from reference optical modeling software.

⋆ The authors thank to the European Commission for funding this work under project DENiM. This project has received funding from the European Union's Horizon 2020 research and innovation programme under grant agreement No 958339. This study was financed in part by the Coordenação de Aperfeiçoamento de Pessoal de Nível Superior – Brasil (CAPES) – Finance Code 88887.578963/2020-00. J. E. Normey-Rico thanks CNPq for financial support, project 304032/2019-0.

10.1016/j.ifacol.2023.10.1839

This paper is divided as follows: Section 2 presents some important aspects of a fresnel collector. Section 3 describes the proposed defocusing algorithm. Section 4 presents the optimization-based defocusing strategy. Section 5 presents the ANFIS defocusing strategy, as well as the training process and training results. Section 6 presents results where simulations are shown that compare the proposed strategies and SolTrace®. Section 7 presents the final remarks of the paper.

2. LINEAR FRESNEL COLLECTOR

The Linear Fresnel Collector (LFC) consists of a structure with some parallel mirrors at the base and an absorber tube above the mirrors, as shown in Figure 1. These mirrors, which can be flat or slightly curved, rotate through their longitudinal axes to make the solar irradiance that is reflected reach the absorber above.

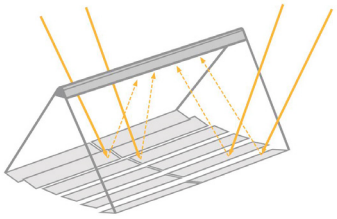

Fig. 1. Representation of the concentration of the solar rays on a Fresnel collector. Adapted from Hahn et al. (2018)

As the apparent movement of the Sun in the sky throughout the day changes the direction from which the predominant solar irradiation reaches the collector, the inclination of the mirrors must be constantly adjusted to maintain the concentration of solar irradiance. This process of adjusting the mirrors due to the movement of the Sun is referred to as solar aiming or solar tracking. To describe the defocusing strategy, it is important to understand how solar tracking is performed considering the total focus of the collector. The simplest aiming strategy consists of making the solar ray that would hit the center of the mirror be reflected on the center of the absorber, as illustrated in Figure 2 (Brandão et al., 2022).

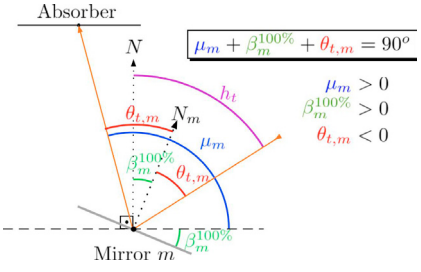

Fig. 2. Representation of simple tracking for some solar hour angle h_t and mirror m. The orange line represents the trajectory of the solar ray that is reflected at the center of the mirror and $\beta_m^{100\%}$ is the mirror's inclination angle while $\theta_{t,m}$ is the transversal projection of the incidence angle on the mirror.

It can be seen that, independently of the transverse projection of the solar hour angle (h_t), the angle between the reflected solar ray and the horizontal plane that passes through the centers of all the mirrors (μ_m) does not change. This angle μ_m is only dependent on the geometry of the collector, and more specifically, depends on the elevation of the absorber (E_{abs}) and the position of the mirror with respect to the absorber's position on the horizontal plane. For a given value of the sun position angle h_t, it is possible to obtain the inclination of mirror m ($\beta_m^{100\%}$) through eq. (1):

$$\beta_m^{100\%} = 45^o - \frac{h_t + \mu_m}{2} \tag{1}$$

Therefore, it is straightforward to compute the angle for all n_{mirr} mirrors of each collector given the solar position (h_t) and the geometry of the collector (μ_m).

3. DEFOCUSING STRATEGY FOR A FRESNEL COLLECTOR

The proposed strategy for defocusing of fresnel collectors consists of changing the focal point of the mirrors in such a way that the amount of irradiance incident on the absorber is equivalent to the percentage defined by the desired focus value (F^{ref}), with respect to the amount of irradiance that the absorber receives when operating the solar tracking with complete focus. This procedure is done by changing the inclination angle of each mirror and is exemplified by Figure 3, where L represents the elevation of the new focal point under the absorber.

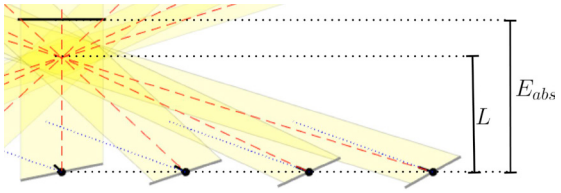

Fig. 3. Illustration of the defocusing strategy on the collector.

The change in focal point can be incorporated into the tracking algorithm by replacing μ_m on (1) with a new angle μ_m^*, such that the reflected rays intercept at height L. This new μ_m^* is given by equation 2.

$$\mu_m^* = \arctan\left(\frac{L.\tan(\mu_m)}{E_{abs}}\right) \tag{2}$$

Although helpful, calculating the mirror inclination angles for a given focus elevation is not sufficient to implement the defocusing strategy, as there is no clear relationship between F^{ref} and the new elevation L. The next sections present two approaches to obtaining the desired focus value.

4. OPTIMIZATION-BASED DEFOCUS

To calculate the focal elevation L that implements the desired focus value F^{ref}, this work initially proposes the use of a precise optical model of the fresnel collector. This model should, given a solar angle h_t and some elevation point L, provide the irradiance at the absorber ($I(h_t, L)$). Defining the complete focus of the collector since it has a focal point coincident with the center of the absorber, the irradiance at this point would be denoted by $I(h_t, E_{abs})$. Thus, it is possible to define the focus state of the collector at any given point as expressed in equation 3:

$$F(h_t, L) = \frac{I(h_t, L)}{I(h_t, E_{abs})} \times 100\% \tag{3}$$

The result from equation 3 provides a relationship between L and F, but it is the inverse of the defocusing implementation issue: for a given solar position h_t and some desired focus value F^{ref},

obtain the focus elevation L that implements the desired focus value. To solve this inverse problem, the optimization problem (4) is proposed , where the cost function (4a) has a quadratic term penalizing the difference between the desired focus (F^{ref}) and the focus value obtained with elevation L ($F(h_t, L)$). The constraint (4b) represents the computation of $F(h_t, L)$ from the optical model, and the constraint (4c) limits the possible elevation of the focal point.

$$\min_{L} (F^{ref} - F(h_t, L))^2 \tag{4a}$$

Subject to

$$F(h_t, L) = f_{model}(h_t, L) \tag{4b}$$

$$0 \leq L \leq E^{abs} \tag{4c}$$

The result of this optimization problem should be the elevation L that implements the desired focus F^{ref}, given an accurate optical model. A schematic of the solution of this optimization problem is given in Figure 4.

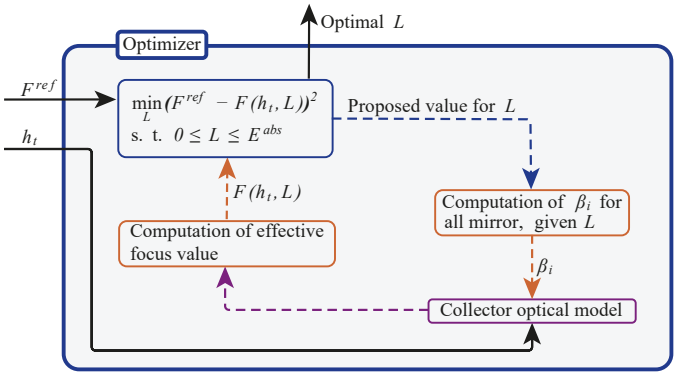

Fig. 4. Representation of the optimization-based defocusing.

The reference optical models which are commonly used to design from solar collectors to whole CSP fields are based on Ray-Tracing techniques. These models use the Monte Carlo method to simulate solar-ray paths and compute their trajectory while reflecting on mirrors and hitting opaque barriers, such as the absorber. One of these Ray-Tracing software is SolTrace® (Wendelin, 2003), which was developed and maintained by the United States National Renewable Energy Laboratory (NREL).

Although it is desirable to use the Ray-Tracing models to solve the optimization problem, it is not practical, as these models have relatively *high computation times* and the topology of the cost function has several local minima and maxima; therefore, it is necessary to use heuristic techniques, such as Particle Swarm Optimization, in order to obtain a solution. These heuristic techniques require large amounts of calls to the objective function and to the Ray-Tracing model, making them impractical for real-time applications. Solving with SolTrace® takes approximately 44 seconds per sample, which may be a high sampling time regarding the overheating issue.

The optical model proposed by Brandão et al. (2022) arises as a second option for this approach, as it has a small computational cost and was validated with SolTrace® for solar tracking. This model, represented by $f_{model}(h_t, L)$, consists of four calculation steps: first, an estimation of the shaded area on each mirror is calculated; then, an estimation of the area of the absorber illuminated by each mirror is done; the third part consists of a correction of the illuminated area of the absorber, considering the shadow cast by the absorber on the mirrors. Finally, the irradiance flux on the absorber is calculated. This model takes as input the absorber elevation and the solar position angles. With this model coupled with the proposed optimization problem, the first proposal for the implementation of the defocusing strategy is complete. The next section presents the other defocusing implementation proposal, now based on a Neurofuzzy approach.

5. NEURO-FUZZY BASED DEFOCUS

Neurofuzzy systems are artificial intelligence (AI) techniques that combine the advantages of fuzzy logic (FL) and artificial neural networks (ANN). The most notable (famous) is the Adaptive Neuro-Fuzzy Inference System (ANFIS) proposed by Jang (1993). It has the capability to construct an input-output mapping based on human knowledge in the form of fuzzy *if-then* rules [1], which can handle imprecise input data (uncertainty).

This paper presents a structure based on an ANFIS to compute the collector focus point that results in a desired defocus value, as represented in Figure 6. In this case, several data points were obtained from SolTrace® in order to train the neurofuzzy network. The SolTrace® software was given a series of values for the solar position (h_t) and elevation (L) and, as previously described, Equation 3 is used in order to obtain reference values for the focus ($F^{ref}(h_t, L)$). These values of h_t, L, and F^{ref} are then used to train the neurofuzzy structure, as described in the next section. The goal is to make this structure provide the correct values of L that implement the desired focus values F^{ref}, given a specific solar angle h_t. Ideally, the ANFIS would be trained with data from an industrial collector, but the instruments necessary for this are not available to the authors.

5.1 Preparation of data

Preliminary work has been done on the data set to train the neurofuzzy-based defocus. The data set is stored in a matrix $\mathbf{D} \in \Re^{n \times m}$, where n is the total number of samples ($n = 44260$) and m represents the number of variables, which in this case are 3. The variables that compose $\mathbf{D}$ are shown in Table 1.

Table 1. Variables composing the data set

Symbol	description	Range		Unit
		Min	Max	
h_t	Transverse solar angle.	0	90	[^{o}]
F^{ref}	Desired focus	0	100	[%]
L	Focus point	0	4	[m]

First, from $\mathbf{D}$ the minimum and maximum of each variable are identified. Subsequently, the data is normalized and the normalized matrix $\mathbf{D}$ is divided into three sets: training, checking, and validation as shown in Figure 5. The learning set is composed of the training and checking sets and has 35408 samples for the learning process and 8852 samples for validation.

A normalization process is added to the learning set using Min-Max feature scaling so that all values fall in the range [0, 1]. The values of each variable have a different scale, which can affect the learning process due to inconsistencies. It is solved by the normalization process, thus avoiding the different nature and

[1] Once the FIS is obtained after completing the ANFIS training, it is possible to add rules. These rules are given by the expert knowledge about the study system.

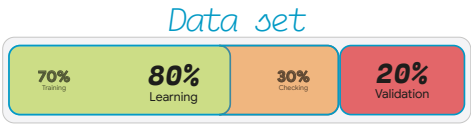

Fig. 5. Organization of available data.

magnitude of the variables, as noted in (Chicaiza et al., 2021, 2022). The new normalized variables are stored in the matrix **Z**.

5.2 Neurofuzzy model obtained

An ANFIS architecture is used to estimate the focus point (L), using the variables h_t and F^{ref} as inlet and (L) as outlet. Thus, a Fuzzy Inference System (FIS) was obtained to estimate the focus point of the collectors. To train the ANFIS network, a data set covering different working points is needed. The ANFIS architecture learning process uses training and test sets. In this process, the ANFIS looks at the normalized RMSE ($nRMSE$) of the training and check set to not overfit only the first set, which would cause the obtained FIS to output inappropriate values for values that have not been seen in the learning process. In this way, it seeks a middle ground where learning is general in both groups.

Initially, a subtractive clustering (SC) method (Chiu, 1994) is applied to obtain the initial structure of the ANFIS, consisting of Gaussian membership functions (MFs) that are the result of the method. That is, SC is used to estimate the number and initial centers of the MFs of the fuzzy rules. The MFs contained *antecedent parameters* of the fuzzy rules and characterized the fuzzy sets (F_{ij}). Furthermore, the output of each rule is a linear combination of input variables summed to a constant term called *consequent parameters*. The final outlet of the ANFIS is obtained by calculating the weighted average of the outcomes of each rule. Thus, a *hybrid learning* method is then applied (Jang, 1993); gradient descent to determine the *antecedent parameters*, i.e., the mean and standard deviation of Gaussian MFs the and least squares to estimate the *consequent parameters* for each epoch or sweep. The parameters of the ANFIS network obtained in the learning process are presented in Table 2.

Table 2. ANFIS parameters

Description	**ANFIS**
MF type:	$Gaussian$
Optimization method:	$hybrid$
Output MF type:	$linear$
FIS	Defocus
Number MFs:	5
Number rules:	5
Influence range	0.6
Epoch number:	2000

The ANFIS network learning process uses some epoch numbers, and the training and checking sets present small errors, indicating that the learning was general. The error indexes obtained in the model learning process and its update time (t_{upd}) are shown in Table 3.

After completion of the ANFIS learning process, a Neurofuzzy $\mathbf{FIS}_{defocus}$ is obtained, which estimates the collector focus point. It consists of a Fuzzy Inference System (FIS) that contains 5 rules of type TS (Takagi and Sugeno, 1985):

$$\texttt{IF } x_1 \texttt{ is } F_{1j} \texttt{ and } x_2 \texttt{ is } F_{2j} \texttt{ and } x_i \texttt{ is } F_{ij} \,,$$
$$\texttt{THEN} : f_j(x) = g_{0j} + g_{1j}x_1 + \cdots + g_{ij}x_i$$

Table 3. nRMSE index obtained of the learning process for the ANFIS and its updating time.

RMSE min of Training & Checking	**ANFIS obtained**
FIS	Defocus
$nRMSE_{Train}(\times 10^{-3})$	8.1552
$nRMSE_{Check}(\times 10^{-3})$	8.8586
$t_{upd}(h)$	0.34

where the description of each of the parameters that make up the rule is extensively described in (Chicaiza et al., 2022). Each rule has *antecedent* and *consequent* parameters. The antecedent parameters consist of membership functions of Gaussian type of each crisp input z_i that form the fuzzy sets. Whereas a first-order polynomial function contains the consequent parameters.

This paper develops a model based on ANFIS. The $\mathbf{FIS}_{defocus}$ describes the performance of the focus point and is shown in Fig.6. The model that estimates the behavior of focus point $\mathbf{FIS}_{defocus}$ is obtained through an ANFIS, it utilizes as inputs the variables mentioned in Table 1, with exception of (L) that is chosen as the model output and, therefore, the variable that the neurofuzzy network must learn.

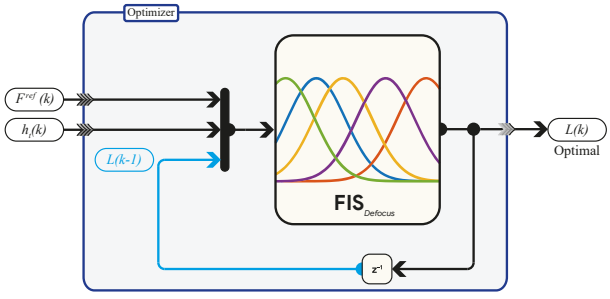

Fig. 6. Neurofuzzy based defocus.

5.3 Validation on Neurofuzzy based defocus

The validation process compares the output of $\mathbf{FIS}_{defocus}$ with the validation data set, that is, a new data set whit 8852 input-output samples. The new data were not used in the learning process of the ANFIS network. Thus, five error indexes were used to compare the FIS output with the actual output data: the arithmetic error mean ($\bar{E}$), standard deviation (Std), Root Mean Square Error($RMSE$), Mean Absolute Percentage Error ($MAPE$) and the coefficient of determination [2] R^2. The error indexes are given by Equations (5)

$$RMSE = \sqrt{\frac{\sum_{i=1}^{N}(x_{i,j} - \hat{x}_{i,j})^2}{N}} \tag{5a}$$

$$MAPE = \frac{\sum_{i=1}^{N} \frac{|(x_{i,j} - \hat{x}_{i,j})|}{x_{i,j}}}{N} \times 100\% \tag{5b}$$

$$R^2 = 1 - \frac{x_{i,j} - \hat{x}_{i,j}}{x_{i,j} - \bar{x}_{i,j}} \tag{5c}$$

where N represents the number of samples in the validation set, $x_{i,j}$ is the actual output value and $\hat{x}_{i,j}$ is the output $\mathbf{FIS}_{defocus}$ obtained and $\bar{x}$ is the mean value of the data. The error indexes

[2] R^2 is a number between 0 and 1, that measures how well a statistical model estimates an outcome. If $R^2 = 0$, the model does not describe the outputs, if $0 < R^2 < 1$, the model partially estimates the outputs, and if $R^2 = 1$ the model perfectly estimates the outputs.

provide information about precision, i.e., how much the error is dispersed.

Figure 7 shows that $\mathbf{FIS}_{defocus}$ is able to follow the real value of the focus point with an error of $0.45e^{-3} \pm 4.5e^{-4}$ $[m]$ as shown in Table 4.

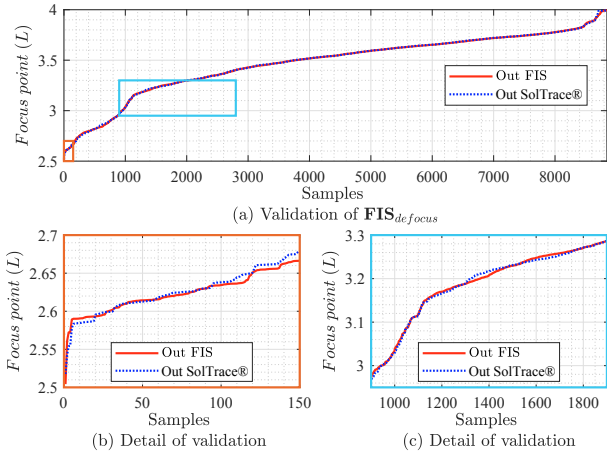

(a) Validation of $\mathbf{FIS}_{defocus}$

(b) Detail of validation

(c) Detail of validation

Fig. 7. (a) $\mathbf{FIS}_{defocus}$ evaluation, FIS output data vs real data. (b) Validation zoom in the first region (orange rectangle). (c) Validation zoom in a second region (cyan rectangle)

Table 4. Validation index of $\mathbf{FIS}_{defocus}$.

Error indexes	$\mathbf{FIS}_{defocus}$ model
$\bar{E}$	$0.45e^{-3}$
Std	$\pm 4.5e^{-4}$
$RMSE$	$4.5e^{-3}$
$MAPE$	0.08%
R^2	0.9998

6. SIMULATIONS AND RESULTS OF THE TWO APPROACHES

This section presents the results for comparing the two proposed defocusing structures when applied to the reference SolTrace® model. The simulations were performed as follows. First, the reference values for the elevation of the focal point (L^{ref}) and the solar hour angle (h_t) were applied to the SolTrace® reference model, resulting in values of the reference focus values (F^{ref}). To evaluate the precision of the defocusing strategies, the reference focus values of SolTrace® are used as inputs in both proposals, and the elevation of the focus point proposed in both cases was compared with the original L^{ref} which contains samples 44200.

The mapping of the optimization-based proposal is presented in Figure 8 , which also presents color-coded information on the irradiance in the absorber. This color code was generated by associating a typical solar irradiation curve with the solar angle data, in order to estimate which points of the mapping represent high irradiation moments of the day.

Regarding the optimization-based strategy, there is noticeable some abnormal behavior for small values of focus, which is due to considering a fresnel collector with an odd number of mirrors. For small focus values, the central mirror will always reflect directly up toward the absorber. Therefore, it will not be possible to have an effective focus that is smaller than the

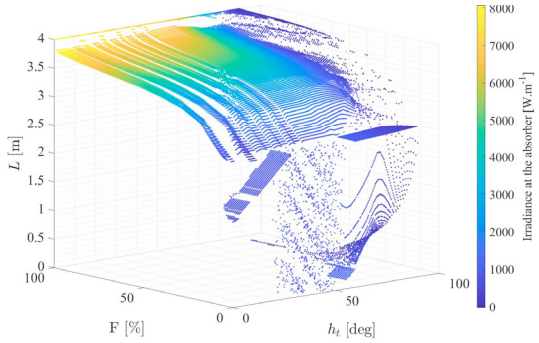

Fig. 8. Mapping of the solution of the defocusing problem for the optimization approach.

contribution of this central mirror. In this situation, the proposed defocusing strategy cannot find an L that implements the desired focus. As this solution will be implemented in future work, the following analysis will only consider $h_t \in [0^o, 60^o]$ and $F \in [10\%, 100\%]$.

To evaluate the precision of the calculated elevations obtained from simulation, Figure 9 presents the results for both proposals and the reference values from SolTrace®.

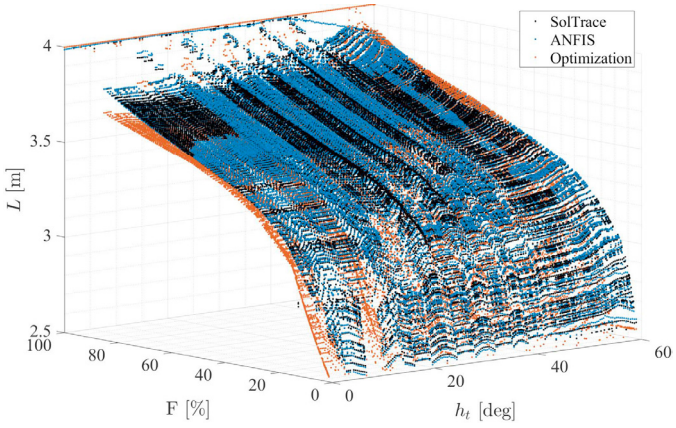

Fig. 9. Comparison of the results for the optimization approach, Neurofuzzy approach and the reference values for the focus.

It is possible to see the highly nonlinear behavior of the defocusing in fresnel collectors. One can also notice that the ANFIS surface seems closer to the reference surface for all points compared to the optimization-based approach. This becomes more evident in Figure 10, where the error for both proposals is shown. It is clearly seen that the ANFIS has approximately a flat and close to zero error throughout the range.

Some performance indices were calculated and presented in Table 5, which reinforces the superior performance of the ANFIS proposal, even when comparing the average execution time for each sample. The error is reduced considerably with respect to the optimization based strategy and does not present problems when using an odd number of mirrors.

Another advantage of both methods is the computation time in comparison to the Soltrace® software (44 s), which would be slow to apply to defocus control signals given the nature of the problem, overheating. The computation time of both methods is less than 1 second, with the ANFIS-based system being the shortest, less than 1 millisecond. In large-scale Fresnel solar plants the computation time is an important factor.

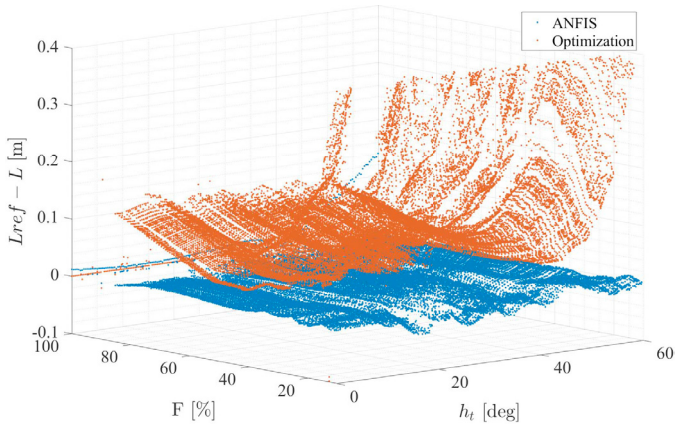

Fig. 10. Comparison of the error for the optimization approach, Neurofuzzy approach.

Table 5. Performance indexes

Index	$\mathbf{FIS}_{defocus}$	Opt. simple model	Opt. SolTrace®
$\bar{E}$	$4.4650e-05$	0.3365	-
$RMSE$	$6.6544e-05$	0.0033	-
$MAPE$	0.2722%	11.3107%	-
R^2	0.9979	0.8344	-
Avg. comp. time (s)	$0.4e^{-3}$	0.4	44

7. CONCLUSION

In this work, an ANFIS network was employed to capture the focus point value of a fresnel collector modeled in the Ray-Tracing software. A fuzzy inference system of first-order recursive 5 rules is obtained once the learning process is completed. In addition, the FIS obtained presents a low error, about the real value of the focus point. It also presented an optimization approach that also implements the proposed defocusing algorithm and showed inferior results compared to ANFIS. The results showed that the proposed defocus strategy based on the optimization algorithm has limitations when using an odd number of mirrors in the fresnel collector. On the other hand, the system ANFIS based approach has shown to have a high performance, with a mean error of $4.4650e-05$, a MAPE of 0.2722% and low computation time. Future works can explore the limitations of the defocusing strategy by considering a change of behavior when only the central mirror is illuminating the absorber. Improving the optimization-based approach with a better optical model is also an interesting research path, as using an FIS model as the optical model of the problem could unite the advantages of both approaches.

ACKNOWLEDGEMENTS

This study was financed in part by Grant PID2019-104149RB-I00 funded by MCIN/AEI/10.13039/501100011033. The authors thank also the European Commission for funding this work under the DENiM project. This project has received funding from the European Union's Horizon 2020 research and innovation programme under grant agreement No 958339. Also, this study was financed in part by the Coordenação de Aperfeiçoamento de Pessoal de Nível Superior – Brasil (CAPES) – Finance Code 88887.578963/2020-00. J. E. Normey-Rico thanks CNPq for financial support, project 304032/2019-0. The authors also thank the National Renewable Energy Laboratory (NREL) for providing a command-line version of SolTrace®.

REFERENCES

Brandão, A., da Costa Mendes, P., and Normey-Rico, J. (2022). Simplified optical model, aiming strategy and partial defocusing strategy for solar fresnel collectors. *Renewable Energy*, 188.

Camacho, E.F., Soria, M.B., Rubio, F.R., and Martínez, D. (2012). *Control of Solar Energy Systems*. Springer London. doi:10.1007/978-0-85729-916-1.

Chicaiza, W.D., Ortiz-Machado, D., Gallego, A.J., Escaño, J.M., Bordons, C., de Andrade, G.A., and Normey-Rico, J.E. (2022). Neuro-fuzzy digital twin of a high temperature generator. *IFAC-PapersOnLine*, 55(9), 466–471. doi:https://doi.org/10.1016/j.ifacol.2022.07.081. 11th IFAC Symposium on Control of Power and Energy Systems CPES 2022.

Chicaiza, W.D., Sánchez, A.J., Gallego, A.J., and Escaño, J.M. (2021). Neuro-fuzzy modelling of a linear fresnel-type solar collector system as a digital twin. In *Joint Proceedings of the 19th World Congress of the International Fuzzy Systems Association (IFSA), the 12th Conference of the European Society for Fuzzy Logic and Technology (EUSFLAT), and the 11th International Summer School on Aggregation Operators (AGOP)*, 242–249. Atlantis Press. doi:https://doi.org/10.2991/asum.k.210827.033.

Chiu, S. (1994). Fuzzy model identification based on cluster estimation. *Journal of the Intelligent and Fuzzy Systems*, 2, 267–278. doi:10.3233/IFS-1994-2306.

Elias, T.d.A., Mendes, P.R.d.C., and Normey-Rico, J.E. (2019). Hybrid predictive controller for overheating prevention of solar collectors. *Renewable Energy*, 136, 535–547.

Escaño, J.M., Sánchez, A.J., Ceballos, M., Gallego, A.J., and Camacho, E.F. (2021). Estimador neuro-borroso, con reducción de complejidad, de las temperaturas de un campo solar cilindro-parabólico. *Revista Iberoamericana de Automática e Informática industrial*, 18(2), 134–145. doi: 10.4995/riai.2020.13261.

Escaño, J.M., Ridao-Olivar, M.A., Ierardi, C., Sánchez, A.J., and Rouzbehi, K. (2020). Driver behavior soft-sensor based on neurofuzzy systems and weighted projection on principal components. *IEEE Sensors Journal*, 20(19), 11454–11462. doi:10.1109/JSEN.2020.2995921.

Hahn, P., Mesquita, M., Pereira, L.T., Knaack, J., and Epp, B. (2018). Energia Termossolar Para a Indústria - Brasil. Technical report, Solar Payback.

Jang, J.S. (1993). Anfis: adaptive-network-based fuzzy inference system. *IEEE Transactions on Systems, Man, and Cybernetics*, 23(3), 665–685. doi:10.1109/21.256541.

Sánchez, A.J., Gallego, A.J., Escaño, J.M., and Camacho, E.F. (2018). Event-based mpc for defocusing and power production of a parabolic trough plant under power limitation. *Solar Energy*, 174, 570–581. doi: https://doi.org/10.1016/j.solener.2018.09.044.

Takagi, T. and Sugeno, M. (1985). Fuzzy identification of systems and its applications to modeling and control. *IEEE Transactions on Systems, Man, and Cybernetics*, SMC-15(1), 116–132. doi:10.1109/TSMC.1985.6313399.

Wendelin, T. (2003). Soltrace: A new optical modeling tool for concentrating solar optics. In *International Solar Energy Conference*. doi:10.1115/ISEC2003-44090.